

Crack roughness and avalanche precursors in the random fuse model

Stefano Zapperi

*INFN UdR Roma 1 and SMC, Dipartimento di Fisica,
Università "La Sapienza", P.le A. Moro 2, 00185 Roma, Italy*

Phani Kumar V.V. Nukala and Srđan Šimunović

Computer Science and Mathematics Division, Oak Ridge National Laboratory, Oak Ridge, TN 37831-6359, USA

We analyze the scaling of the crack roughness and of avalanche precursors in the two dimensional random fuse model by numerical simulations, employing large system sizes and extensive sample averaging. We find that the crack roughness exhibits anomalous scaling, as recently observed in experiments. The roughness exponents (ζ , ζ_{loc}) and the global width distributions are found to be universal with respect to the lattice geometry. Failure is preceded by avalanche precursors whose distribution follows a power law up to a cutoff size. While the characteristic avalanche size scales as $s_0 \sim L^D$, with a universal fractal dimension D , the distribution exponent τ differs slightly for triangular and diamond lattices and, in both cases, it is larger than the mean-field (fiber bundle) value $\tau = 5/2$.

I. INTRODUCTION

Understanding the scaling properties of fracture in disordered media represents an intriguing theoretical problem with some technological implications [1]. Experiments have shown that in several materials under different loading conditions the fracture surface is self-affine [2] and the out of plane roughness exponent displays a universal value irrespective of the material studied [3]. In particular, experiments have been done in metals [4], glass [5], rocks [6] and ceramics [7], covering both ductile and brittle materials.

It was later shown that the roughness exponent conventionally measured describes only the local properties, while the fracture surface instead exhibits anomalous scaling [10]: the *global* exponent describing the scaling of the crack width with the sample size is larger than the local exponent measured on a single sample [11]. It is thus necessary to define two roughness exponents a global (ζ) and a local ζ_{loc} . Only the latter appears to be universal with a value $\zeta_{loc} \simeq 0.8$ [3]. For the purpose of this paper, it is important to mention that experiments performed in quasi two-dimensional geometries, in wood [8] or paper [9], yield a self-affine exponent close to the minimum energy surface result $\zeta_{loc} = 2/3$.

Scaling is also observed in acoustic emission experiments, where the distribution of pulses decays as a power law over several decades. Experimental observations have been reported for several materials such as wood [12], cellular glass [13], concrete [14] and paper [15], but universality in the scaling exponents does not appear to be present.

The experimental observation of scaling behavior suggests an interpretation in terms of critical phenomena, but a complete theoretical explanation has not been found. The motion of a crack front has been modeled as a deformable line pushed by the external stress through a random toughness landscape. Deformation of the crack surface is caused by disorder and opposed by the elas-

tic stresses. In certain conditions, the problem can be directly related to models and theories of interface depinning in random media and the roughness exponent computed by numerical simulations and renormalization group calculations [16, 17]. Unfortunately, the numerical agreement between this theoretical approach and experiments is quite poor [18, 19, 20].

One aspect missing from the crack line model is the nucleation of voids in front of the main crack, an effect that has been shown to occur experimentally [21]. In this perspective, disordered lattice models appear to be more appropriate to describe the phenomenon. In these models the elastic medium is described by a network of springs with random failure thresholds. In the simplest approximation of a scalar displacement, one recovers the random fuse model (RFM) where a lattice of fuses with random threshold are subject to an increasing external voltage [22, 23, 24, 25, 26]. The model has been numerically simulated to obtain the roughness of the fracture surface in two [27, 28] and three dimensions [29, 30]. The measured roughness exponents turn out to be similar to the one describing a minimum energy surface (or a directed polymer in $d = 2$) suggesting that crack formation occurs by an optimization process.

In addition, the fracture of the RFM is preceded by avalanches of failure events [31, 32, 33]. These are reminiscent of the acoustic emission activity observed in experiments. The distribution of avalanche sizes (i.e. the number of bonds participating in an avalanche) follows a power law. In previous simulations the exponent resulted to be close to $\tau = 5/2$, the value expected in the fiber bundle model (FBM) [34, 35]. In the FBM, load is redistributed equally in all the fibers, representing thus a sort of mean-field limit of the RFM [32]. The load transfer in the RFM is long-ranged and is thus possible that RFM and FBM display universal behavior [36]. An intermediate case is provided by FBM with long-range (power law) load transfer [37]: the difference with the RFM lies in the anisotropic current transfer function [36].

Numerical simulation of fracture in the RFM is often hampered by the high computational cost associated with solving a new large set of linear equations every time a new lattice bond is broken. Previously, this fact has restricted the simulations to smaller lattice sizes and fewer statistical sampling of data, thereby affecting the quality of the results. Here, thanks to the new algorithm discussed in Ref. [26], we report results of numerical simulations for large two-dimensional lattices (triangular and diamond) with extended statistics. We concentrate on the roughness of the final crack and the avalanche statistics preceding failure.

Using local and global measurements for the roughness we find that cracks in the RFM follow anomalous scaling [10]. The local roughness exponent is found to be in the range $\zeta_{loc} = 0.70 - 0.75$, while the global exponent falls in the range $\zeta = 0.80 - 0.85$. Although the difference between ζ and ζ_{loc} is small it appears to be systematic. The results are obtained using the local width and the power spectrum methods and appear to be universal with respect to the lattice type. As a further test, we compute the width distribution that can be collapsed into a unique curve for different lattice sizes and types [38].

Next, we consider the distribution of avalanche sizes. The avalanche signal is not stationary and as the current is raised avalanches becomes larger and larger. The last avalanches, producing the failure of the sample, is typically much larger than the previous one and it follows a normal distribution with a typical value scaling as $s_m \sim L^{1.4}$. Preceding avalanches are distributed as a power law with a cutoff increasing with the current. Integrating the distribution over all the values of the current, we find a power law up to a cutoff, scaling with the lattice size as L^D , where $D \simeq 1.18$ does not depend on the lattice type and is thus universal. The exponent describing the decay of the distribution is found instead to differ for triangular and diamond (square lattice with 45 degrees inclined bonds to the bus bars) lattices with a value which is always larger than the FBM value $\tau = 5/2$.

The paper is organized as follows: in section II we define the model, in section III we report the results on the crack roughness and section IV is devoted to the avalanche statistics and in section V we conclude.

II. THE RANDOM FUSE MODEL

In the RFM [22], the lattice is initially fully intact with bonds having the same conductance and random breaking thresholds t , uniformly distributed between 0 and 1. The burning of a fuse occurs irreversibly, whenever the electrical current in the fuse exceeds breaking threshold t of the fuse. Periodic boundary conditions are imposed in the horizontal direction to simulate an infinite system and a constant voltage difference, V , is applied between the top and the bottom of lattice system bus bars. Numerically, a unit voltage difference, $V = 1$, is set between the bus bars and the Kirchhoff equations are solved to

determine the current flowing in each of the fuses. Subsequently, for each fuse j , the ratio between the current i_j and the breaking threshold t_j is evaluated, and the bond j_c having the largest value, $\max_j \frac{i_j}{t_j}$, is irreversibly removed (burnt). The current is redistributed instantaneously after a fuse is burnt implying that the current relaxation in the lattice system is much faster than the breaking of a fuse. Each time a fuse is burnt, it is necessary to re-calculate the current redistribution in the lattice to determine the subsequent breaking of a bond. The process of breaking of a bond, one at a time, is repeated until the lattice system fails completely. At this point we analyze the morphology of the spanning crack.

The same breaking sequence is obtained by raising the voltage difference or the total current at an infinitesimal rate. Doing this one can identify an avalanche as the set of fuses breaking between two successive increases of the voltage (or the current). In this paper, we follow Ref. [32], considering only current driven avalanches. The avalanche size is defined as the number of fuses in an avalanche.

Simulations are performed on two dimensional triangular and diamond lattices of linear sizes going from $L = 16$ up to $L = 1024$ (for the triangular lattice) or up to $L = 256$ (for the diamond lattice). The total number of bonds in the lattice is given by $N = (3L + 1)(L + 1)$ for the triangular lattice and $N = 2L(L + 1)$ for the diamond lattice. Several results discussed in the following sections could only be obtained under an extensive statistical sampling. Due to numerical limitations this could not be achieved for the largest lattice sizes. Each numerical simulation was performed on a single processor of *Eagle* (184 nodes with four 375 MHz Power3-II processors) supercomputer at the Oak Ridge National Laboratory. The statistically independent N_{config} number of configurations were simulated simultaneously on number of processors available for computation (the actual values of N_{config} is reported in Table 1 of Ref. [40]).

III. CRACK ROUGHNESS

After the sample has failed we identify the final crack, an example of which is reported in Fig. 1. The cracks typically display some limited amount of dangling ends and overhangs. We remove them and obtain a single valued crack line y_x , where the values of $x \in [0, L]$ depend on the underlying lattice topology. Several methods have been devised to characterize the roughness of an interface and their reliability has been tested against synthetic data [41]. If the interface is self-affine all the methods should yield the same result in the limit of large samples. For instance the local width, $w(l) \equiv \langle \sum_x (y_x - (1/l) \sum_X y_X)^2 \rangle^{1/2}$, where the sums are restricted to regions of length l and the average is over different realizations, should scale as $w(l) \sim l^\zeta$ for $l \ll L$ and should saturate to a value $W = w(L) \sim L^\zeta$ corresponding to the global width. The power spec-

trum $S(k) \equiv \langle \hat{y}_k \hat{y}_{-k} \rangle$, where $\hat{y}_k \equiv \sum_x y_x \exp i(2\pi x k/L)$, should decay as $S(k) \sim k^{-(2\zeta+1)}$.

While numerical estimates with the two methods above could yield different results, it is also possible that the scaling is anomalous[10]. This has been observed not only in various growth models [10] but also in fracture surfaces in granite and wood samples[11]. Anomalous scaling implies that the exponent describing the system size dependence of the surface *differs* from the local exponent measured for a fixed system size L . In particular, the local width scales as $w(l) \sim l^{\zeta_{loc}} L^{\zeta - \zeta_{loc}}$, so that the global roughness W scales as L^ζ with $\zeta > \zeta_{loc}$. Consequently, the power spectrum scales as $S(k) \sim k^{-(2\zeta_{loc}+1)} L^{2(\zeta - \zeta_{loc})}$.

Previous measurements of the crack roughness in the two-dimensional random fuse model have been obtained studying the global roughness and anomalous roughness could not be detected. Here, thanks to the improved statistics and system size range, we reveal clear indication of anomalous scaling behavior. In Fig. 2 we report the local width for diamond and triangular lattices for different sizes L . The curves for different system sizes are not overlapping even for $l \ll L$ as expected for anomalous scaling. The global width scales with an exponent $\zeta = 0.80 \pm 0.02$ and $\zeta = 0.83 \pm 0.02$ for diamond and triangular lattices respectively. On the other hand the local width increases with a smaller exponent, that can be estimated for the larger system sizes as $\zeta_{loc} \simeq 0.7$ for both lattices. A more precise value of the exponents is obtained from the power spectrum, which is expected to yield more precise estimates. Fig. 3 reports the data collapse of the power spectra for different system sizes. The data are collapsed using $\zeta - \zeta_{loc} = 0.1$ and $\zeta - \zeta_{loc} = 0.13$ for diamond and triangular lattices, respectively. A fit of the power law decay of the spectrum yields instead $\zeta_{loc} = 0.7$ and $\zeta_{loc} = 0.74$ for the two lattices, implying $\zeta = 0.8$ and $\zeta = 0.87$. The results are close to the real space estimates and we can attribute the differences to the bias associated to the methods employed [41].

Although the value of $\zeta - \zeta_{loc}$ is small, it is significantly larger than zero so that we would conclude that anomalous scaling is present. While the local exponent is close to the directed polymer value $\zeta = 2/3$, the global value is much higher. In addition, the presence of anomalous scaling would invalidate universality between directed polymers and fracture: directed polymers should not display anomalous scaling. As for the question of universality of the random fuse model crack roughness exponents, the values measured above are quite close to each other and the differences could be due to size effects. In order to have a further confirmation of this, we have analyzed the distribution $P(W)$ of the crack global width. This distribution has been measured for various interfaces in models and experiments and typically rescales as [38]

$$P(W) = P(W/\langle W \rangle)/\langle W \rangle, \quad (1)$$

where $\langle W \rangle \sim L^\zeta$ is the average global width. The crack width distribution has been measured for the random

fuse model with limited statistical sampling. We show in Fig. 4 that the distributions can be collapsed well using Eq. 1 for diamond and triangular lattices. The plot in Fig. 5 shows that the collapsed distribution for the two lattices superimpose, which we consider as a further indication of universality. Finally, the width distributions are well fit by a log-normal distribution as shown in Fig. 5.

IV. AVALANCHES

The qualitative behavior of the avalanche statistics is well understood in FBM, which can be solved exactly representing a mean-field version of the RFM [32]. The FBM can be formulated as a parallel set of fuses, with random breaking threshold, under a constant applied current I . Thus each fuse carry the same current $f_i = I/n$, where n is the number of intact fuses. The FBM has been solved exactly and it is known that there is a critical value $I = I_c$ at which the bundle fails through a macroscopic avalanche. For $I < I_c$ fuses burn in smaller avalanches, whose sizes are distributed as

$$p(s, I^*) = s^{-\gamma} h(-s/s^*), \quad (2)$$

with $\gamma = 3/2$, and $h(x)$ is a cutoff function. The cutoff size s^* increases with the current and close to I_c diverges as $s^* \sim (I_c - I)^{1/\sigma}$ with $\sigma = 1$. One can then integrate the distribution over all the values of the current, obtaining an $P(s) \sim s^{-\tau}$ with $\tau = \gamma + \sigma = 5/2$.

Here we study the statistical properties of the avalanches in the RFM. We can use the scaling laws established for the FBM as a reference, with additional complications due to finite size effects. In Fig. 6 we report the integrated avalanche distribution obtained for different lattice sizes. We observe a power law decay culminating with a peak at large avalanche sizes. As in the FBM, the peak is due to the last catastrophic event which can thus be considered as an outlier and analyzed separately. When the last avalanche is removed from the distribution the peak disappears (see Fig. 6).

The avalanche size distribution, once the last event is excluded, is a power law followed by an exponential cutoff at large avalanche sizes. The cutoff size s_0 is increasing with the lattice size, so that we can describe the distribution by a scaling form

$$P(s, L) = s^{-\tau} g(s/L^D), \quad (3)$$

where D represents the fractal dimension of the avalanches. To take into account the different lattice geometries, it is convenient to express scaling plots in terms of N rather than L

$$P(s, N) = s^{-\tau} g(s/N^{D/2}). \quad (4)$$

A powerful method to test these scaling laws, extracting τ and D , is provided by the moment analysis [39]. We compute the q th moment of the distribution $M_q \equiv \langle s^q \rangle$

and plot it as a function of N . This defines an exponent σ_q as $M_q \sim N^{\sigma_q}$. If the data follow Eq. 4 then $\sigma_q = 0$ for $q < \tau - 1$ and $\sigma_q = D(q + 1 - \tau)/2$ for $q > \tau - 1$. In order to measure σ_q , we consider lattice sizes from $L = 16$ to $L = 128$ since the statistical sampling for larger sizes is not adequate to estimate correctly the cutoff s_0 . The data displayed in Fig. 7 show that indeed σ_q is linear in q at large q and vanishes for small q . The curves for triangular and diamond lattice do not coincide: the two lines are parallel, indicating that D is the same, but the intersection with the x axis differs. By a linear fit we obtain $\tau = 2.75$ and $D/2 = 0.59$ for diamond lattices and $\tau = 3.05$ and $D/2 = 0.585$ for triangular lattices. To confirm these results we perform a data collapse using the estimated values of the exponents and result is reported in Fig. 8. While the data collapse for diamond lattice is nearly perfect, some deviations are noticeable for the triangular lattice.

From the analysis discussed above, we would conclude that the avalanche fractal D dimension is universal, but a significant difference is present for the exponent τ . This difference could be due to lattice finite size effect as we will discuss later. In addition, the value of τ appears to be larger than the mean-field result $\tau = 5/2$ obtained in the FBM. On the basis of less accurate results, it was conjectured in Ref. [32] that avalanches in the random fuse model are ruled by mean-field theory. The present results seem to rule out this possibility.

So far we have considered avalanche statistics integrating the distribution over all the values of the current. We have noticed, however, that the avalanche signal is not stationary: as the current increases so does the avalanche size. In particular, the last avalanche is much larger than the others. Its typical size grows as $s_m \sim N^b$, with $b \simeq 0.7$ see Fig. 4 of Ref. [40] (s_m is referred as $n_f - n_p$ in that paper), while the distribution is approximately Gaussian as shown from the data collapse reported in Fig. 9

In Fig. 10 we report the distribution of avalanche sizes sampled at different values of the current I . For each sample, we normalize the current by its peak value I_c and divide the $I^* = I/I_c$ axis into 20 bins. We then compute the avalanche size distribution $p(s, I^*)$ for each bin and average over different realizations of the disorder. In Fig. 10 we report this distribution for a diamond lattice of size $L = 128$. The distribution follows a law of the type

$$p(s, I^*) = s^{-\gamma} \exp(-s/s^*), \quad (5)$$

with $\gamma \simeq 1.9$, while in the FBM $\gamma = 3/2$.

In order to extract the dependence of the cutoff s^* on I^* , we compute the second moment of the distribution $\langle s^2 \rangle$. According to Eq. 5, this should scale as $\langle s^2 \rangle = (s^*)^{3-\gamma}$. Assuming that for large systems $s^* \sim (1 - I^*)^{-1/\sigma}$ (in the FBM this holds with $\sigma = 1$), we expect that the singularity is rounded at small L as

$$s^* \sim \frac{L^D}{(1 - I^*)^{1/\sigma} L^D + C}, \quad (6)$$

where C is a constant. The second moment can be collapsed very well under this finite size scaling assumption with $1/\sigma = 1.4$ and $D = 1.18$ as shown in Fig. 11 for the diamond lattice. The data collapse is consistent with the finite size scaling of the integrated distribution with a cutoff increasing as $s_0 \sim L^D$. In fact integrating Eq. 5 we obtain

$$P(s, L) \sim s^{-(\gamma+\sigma)} \exp[-sC/L^D]. \quad (7)$$

which implies $\tau = \gamma + \sigma$. Using the estimated data we would obtain $\gamma + \sigma \simeq 2.6$ in reasonable agreement with the integrated distribution result $\tau = 2.75$.

We have performed the same analysis for the triangular lattice, where we find similar scaling laws with $\gamma \simeq 2$ and $\sigma = 1.3$. This would give $\tau = 2.7$ that is quite off from the integrated distribution result $\tau = 3.05$. These variations could indicate some systematic error present in the triangular lattice results. We notice that while in the diamond lattice, at the beginning of the simulation, all fuses carry the same current, in the triangular lattice only two thirds of the fuses carry a current. As fuses break the current is redistributed becoming inhomogeneous so that at breakdown this lattice effect should not be visible. In fact scaling exponents computed at failure, like the roughness exponent or the avalanche cutoff, do not depend on the lattice type. On the other hand, the integrated avalanche distribution is affected by the entire rupture process and the estimated exponent could thus be biased.

V. CONCLUSIONS

In this paper we have revised some statistical properties of fracture in the random fuse model using an improved statistical sampling and larger lattices than what previously done in the past. We have analyzed the roughness of the final crack for diamond and triangular lattices. The local roughness exponent is found to be $\zeta_{loc} = 0.72 \pm 0.03$ and appears to be different from the global roughness exponent which turns out to be $\zeta = 0.83 \pm 0.04$. These results have been obtained from the local width and the power spectrum methods and the error bars above merely represent the spread of the estimated exponents using various methods and lattice types. The data suggest that anomalous scaling is present, as already found in fracture experiments [11]. The numerical value of the local exponent is in reasonable agreement with the experiments on quasi two-dimensional materials [8, 9]. As a further test for universality, we have also evaluated the width distribution [38] that can be collapsed into a single curve for different lattice sizes and types. From the theoretical point of view, our results seem to exclude the minimum energy surface exponent of $\zeta = 2/3$. While the local exponent is close to that value, the global exponent is definitely higher. In addition anomalous scaling is not expected for that model. Thus the origin of measured roughness

exponents and its theoretical explanation remains still open.

We have also analyzed the scaling of failure precursors, computing the distribution of avalanche sizes. The extensive statistical sampling employed allowed us to observe a power law decay up to a cutoff, which was not visible in previous simulations [31, 32]. The cutoff size is found to increase with the lattice size as $s_0 \sim L^D$, where the exponent $D \simeq 1.18$ depends very little on the lattice size. It is interesting to notice that for self-affine lines of roughness, ζ , one expects a fractal dimension $D = 2 - \zeta$ [42]. If we plug into this expression the global roughness results obtained above for the final crack, we obtain $D \simeq 1.13 - 1.20$. This could imply that the geometrical properties of the precursors are the same as that of the final crack. On the other hand, the exponent of the avalanche size distribution displays significant variations with the lattice type (i.e. $\tau = 2.75$ and $\tau = 3.05$ for diamond and triangular lattices respectively) and is significantly different from the mean-field result $\tau = 5/2$ that was conjectured to be valid in [32].

The integrated avalanche distribution is due to the convolution of the avalanche distribution measured at different values of the current. We have shown that the non-integrated distribution is given by a power law with an

exponential cutoff that increases with the current. The combined analysis of the distribution with respect to current and lattice size can be performed using finite size scaling. The behavior of the model is similar to the FBM, as noticed in Ref. [32], but the numerical values of the exponents change. For the diamond lattice we estimate $\gamma = 1.9$ and $\sigma = 1.4$, while the FBM yields $\gamma = 3/2$ and $\sigma = 1$. Similar results hold for the triangular lattice although the scaling there appears to be less clear.

It would be interesting to understand these results theoretically by the renormalization group, using the mean-field theory as a reference. Steps in this direction have been made in Ref. [36] but the complicated (dipolar) structure of the current redistribution function makes the problem very hard to deal with. Long-range interactions appear to be crucial in the appearance of scaling behavior, since local fracture models yield abrupt failure without large precursors [43]. A similar scenario is characteristic of first-order phase transitions occurring close to a spinodal. In that case spinodal scaling is only seen in mean-field or with long range interaction [44]. The fact that the exponents deviate from mean-field ones, however, calls for a more detailed understanding of the origin of scaling in the random fuse model.

-
- [1] H. J. Herrmann and S. Roux (eds.), *Statistical Models for the Fracture of Disordered Media*, (North-Holland, Amsterdam, 1990). B. K. Chakrabarti and L. G. Benguigui, *Statistical physics of fracture and breakdown in disordered systems* (Oxford Univ. Press, Oxford, 1997).
 - [2] B. B. Mandelbrot, D. E. Passoja, and A. J. Paullay, *Nature* (London) **308**, 721 (1984).
 - [3] For a review see E. Bouchaud, *J Phys. C* **9**, 4319 (1997)
 - [4] K.J. Maloy, A. Hansen, E.L. Hinrichsen, and S. Roux, *Phys. Rev. Lett.* **68**, 213 (1992); E. Bouchaud, G. Lapasset, J. Planés, and S. Navéas, *Phys. Rev. B* **48**, 2917 (1993).
 - [5] P. Daguer, B. Nghiem, E. Bouchaud, and F. Creuzet, *Phys. Rev. Lett.* **78**, 1062 (1997).
 - [6] J. Schmittbuhl, S. Roux, and Y. Berthaud, *Europhys. Lett.* **28**, 585 (1994). J. Schmittbuhl, F. Schmitt, and C. Scholz, *J. Geophys. Res.* **100**, 5953 (1995).
 - [7] J.J. Mecholsky, D.E. Passoja, and K.S. Feinberg-Ringel, *J. Am. Ceram. Soc.* **72**, 60 (1989).
 - [8] T. Engoy, K. J. Maloy, A. Hansen, and S. Roux, *Phys. Rev. Lett.* **73**, 834 (1994).
 - [9] J. Kertész, V. K. Horváth, and F. Weber, *Fractals* **1**, 67 (1993). J. Rosti, L.I. Salminen, E.T. Seppälä, M.J. Alava and K.J. Niskanen, *Eur. Phys. J. B* **19**, 259 (2001); L.I. Salminen, M.J. Alava and K.J. Niskanen *ibid* **32**, 369 (2003).
 - [10] J. M. López, M. A. Rodríguez, and R. Cuerno, *Phys. Rev. E* **56**, 3993 (1997).
 - [11] J. M. López and J. Schmittbuhl, *Phys. Rev. E* **57**, 6405 (1998). S. Morel, J. Schmittbuhl, J. M. López, and G. Valentin, *Phys. Rev. E* **58**, 6999 (1998).
 - [12] A. Garcimartín, A. Guarino, L. Bellon and S. Ciliberto, *Phys. Rev. Lett.* **79**, 3202 (1997); A. Guarino, A. Garcimartín and S. Ciliberto, *Eur. Phys. J. B* **6**, 13 (1998).
 - [13] C. Maes, A. Van Moffaert, H. Frederix and H. Strauven, *Phys. Rev. B* **57**, 4987 (1998).
 - [14] A. Petri, G. Paparo, A. Vespignani, A. Alippi and M. Costantini, *Phys. Rev. Lett.* **73**, 3423 (1994).
 - [15] L.I. Salminen, A.I. Tolvanen, and M. J. Alava, *Phys. Rev. Lett.* **89**, 185503 (2002).
 - [16] T. Nattermann, S. Stepanow, L. H. Tang, and H. Leschhorn, *J. Phys. II (France)* **2**, 1483 (1992).
 - [17] O. Narayan and D. S. Fisher, *Phys. Rev. B* **48**, 7030 (1993).
 - [18] S. Ramanathan, D. Ertas, and D. S. Fisher, *Phys. Rev. Lett.* **79**, 873 (1997).
 - [19] J. Schmittbuhl, S. Roux, J. P. Vilotte, and K. J. Måløy, *Phys. Rev. Lett.* **74**, 1787 (1995); A. Tanguy, M. Gounelle and S. Roux, *Phys. Rev. E* **58**, 1577-1590, (1998).
 - [20] S. Ramanathan and D. S. Fisher, *Phys. Rev. Lett.* **79**, 877 (1997); *Phys. Rev. B* **58**, 6026 (1998).
 - [21] F. Célarie et al., *Phys. Rev. Lett.* **90** 075504 (2003).
 - [22] L. de Arcangelis, S. Redner, and H. J. Herrmann, *J. Phys. (Paris) Lett.* **46** 585 (1985).
 - [23] B. Kahng, G. G. Batrouni, S. Redner, L. de Arcangelis and H. J. Herrmann, *Phys. Rev. B* **37**, 7625 (1988).
 - [24] L. de Arcangelis, A. Hansen, H. J. Herrmann, and S. Roux, *Phys. Rev. B*, **40**, 877 (1989).
 - [25] A. Delaplace, G. Pijaudier-Cabot, and S. Roux, *Journal of Mechanics and Physics of Solids*, **44**, 99 (1996).
 - [26] P. K. V. V. Nukala, and S. Simunovic, *J. Phys. A: Math. Gen.* **36**, 11403 (2003).
 - [27] A. Hansen, E. L. Hinrichsen, and S. Roux, *Phys. Rev.*

- Lett. **66**, 2476 (1991).
- [28] E. T. Seppälä, V. I. Räisänen, and M. J. Alava Phys. Rev. E **61**, 6312 (2000)
- [29] G. G. Batrouni and A. Hansen, Phys. Rev. Lett. **80**, 325 (1998).
- [30] V. I. Räisänen, E. T. Seppälä, M. J. Alava, and P. M. Duxbury, Phys. Rev. Lett. **80**, 329 (1998).
- [31] A. Hansen and P. C. Hemmer, Phys. Lett. A **184**, 394 (1994).
- [32] S. Zapperi, P. Ray, H. E. Stanley, and A. Vespignani, Phys. Rev. Lett. **78**, 1408 (1997); Phys. Rev. E **59**, 5049 (1999).
- [33] V. I. Räisänen, M. J. Alava, R. M. Nieminen, Phys. Rev. B, **58**, 14288 (1998).
- [34] H. A. Daniels, Proc. Roy. Soc. London **A183**, 405 (1945); S. L. Phoenix and H. M. Taylor, Adv. Appl. Prob. **5**, 200 (1973).
- [35] P. C. Hemmer and A. Hansen, J. Appl. Mech. **59**, 909 (1992); M. Kloster, A. Hansen and P. C. Hemmer Phys. Rev E **56**, 2615 (1997).
- [36] M. Barthelemy, R. da Silveira and H. Orland, Europhys. Lett. **57** 831 (2002).
- [37] R. C. Hidalgo, Y. Moreno, F. Kun, and H. J. Herrmann Phys. Rev. E **65**, 046148 (2002).
- [38] G. Foltin, K. Oerding, Z. Rácz, R.L. Workman, and R.K.P. Zia, Phys. Rev. E **50**, R639 (1994); M. Plischke, Z. Rácz, and R.K.P. Zia, Phys. Rev. E **50**, 3589 (1994); Z. Rácz and M. Plischke, Phys. Rev. E **50**, 3530 (1994); T. Antal, M. Droz, G. Györgyi, and Z. Rácz, Phys. Rev. Lett. **87**, 240601 (2001); Phys. Rev. E **65**, 046140 (2002); A. Rosso, W. Krauth, P. Le Doussal, J. Vannimenus, and K. J. Wiese Phys. Rev. E **68**, 036128 (2003).
- [39] M. De Menech, A. L. Stella and C. Tebaldi, Phys. Rev. E **58**, R2677 (1998); A. Chessa, A. Vespignani and S. Zapperi, Comp. Phys. Comm. **121-122**, 299 (2000).
- [40] P. K. V.V. Nukala, S. Simunovic and S. Zapperi, preprint cond-mat/0311284.
- [41] J. Schmittbuhl, J. P. Vilotte, and S. Roux Phys. Rev. E **51**, 131-147 (1995).
- [42] B. B. Mandelbrot, Physica Scripta **32**, 257 (1985).
- [43] F. Kun, S. Zapperi and H. J. Herrmann, Eur. Phys. J. B **17**, 269 (2000).
- [44] C. Unger and W. Klein, Phys. Rev. B **29**, 2698 (1984); *ibidem* **31**, 6127 (1985). For a review see L. Monette, Int. J. of Mod. Phys B **8**, 1417 (1994).

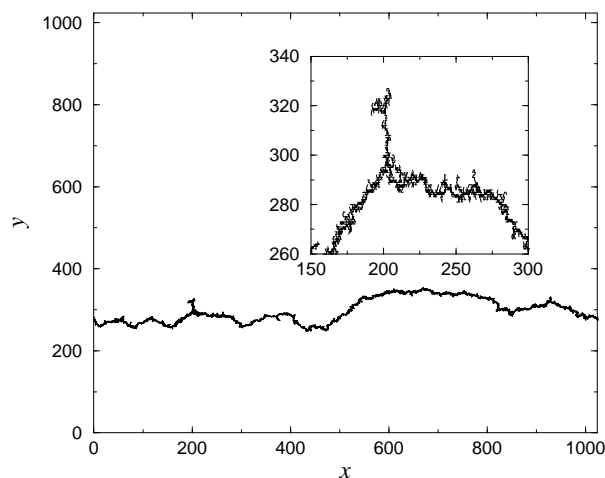


FIG. 1: The final crack in a triangular lattice of size $L = 1024$ (a detail is shown in the inset). The crack displays some dangling ends and overhangs that are removed before performing the analysis.

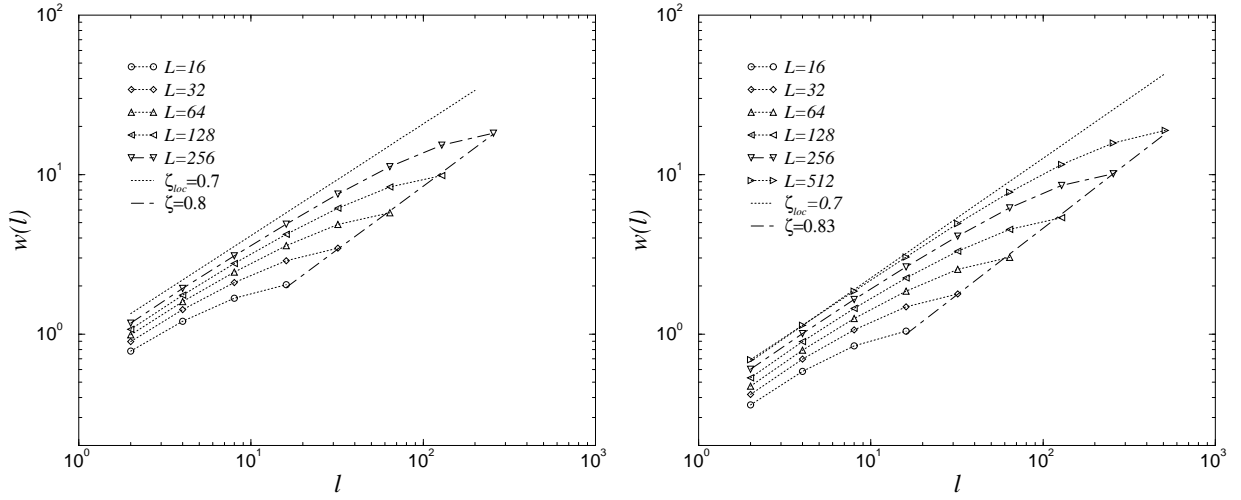


FIG. 2: The local width $w(l)$ of the crack for different lattice sizes in log-log scale. A line with the local exponent $\zeta_{loc} = 0.7$ is plotted for reference. The global width displays an exponent $\zeta > \zeta_{loc}$. Data are shown for diamond (left) and triangular (right) lattices.

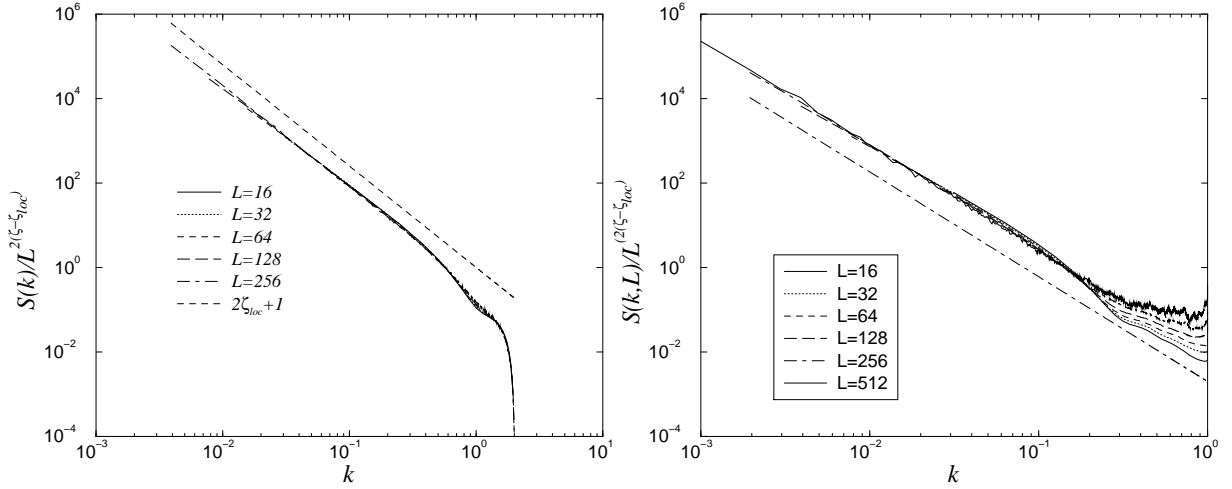


FIG. 3: The power spectrum of the crack $S(k, L)$ for different lattice sizes in log-log scale. The slope defines the local exponent as $-(2\zeta_{loc} + 1)$. The spectra for all of the different lattice sizes can be collapsed indicating anomalous scaling. Data are shown for diamond (left) and triangular (right) lattices.

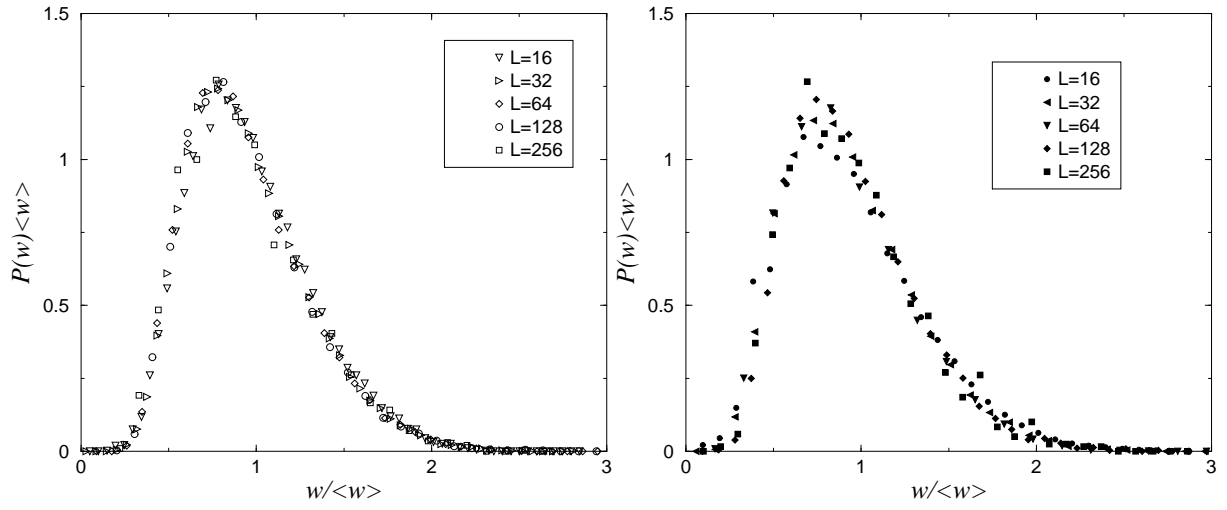


FIG. 4: The distribution of crack width for different lattice sizes can be collapsed using their average value. Data are shown for diamond (left) and triangular (right) lattices.

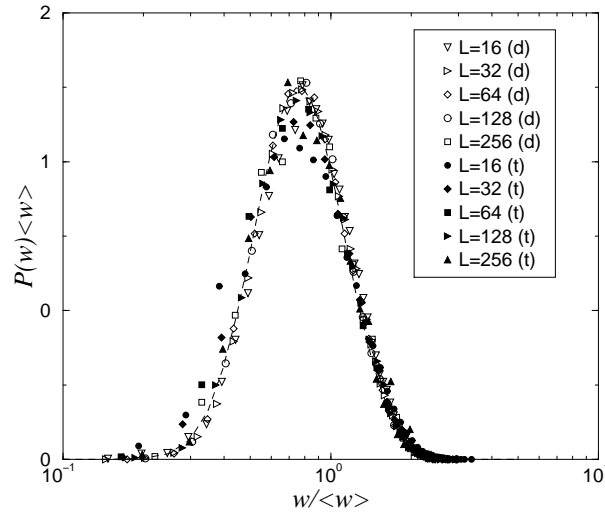


FIG. 5: The distribution of crack width is universal for diamond and triangular lattices since all the curves can be collapsed together. A fit with a lognormal distribution is shown by a dashed line.

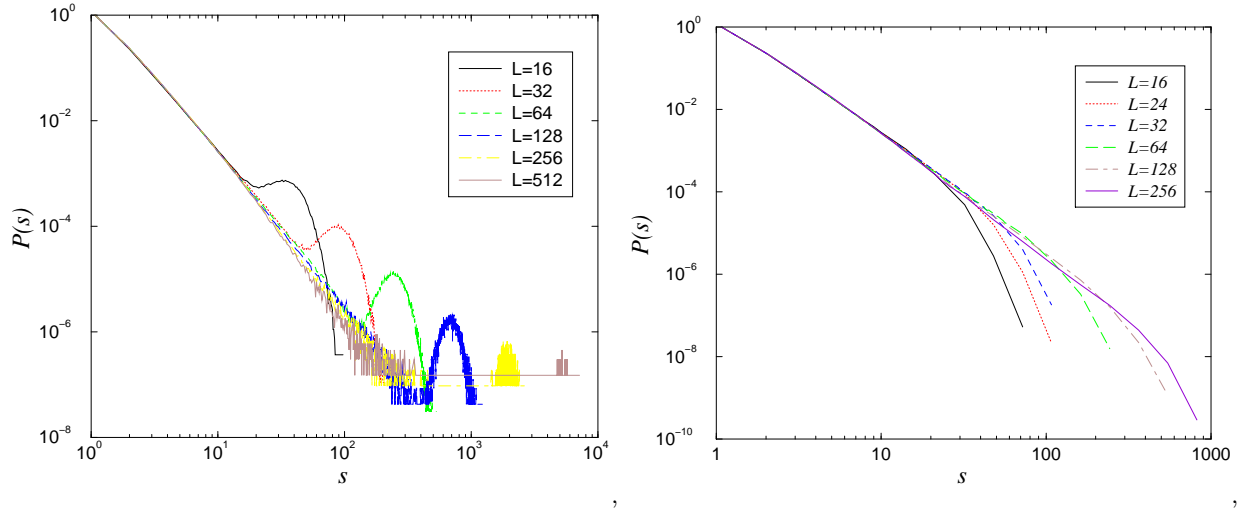


FIG. 6: The distribution of avalanche sizes for triangular lattices of different sizes. The peak at large size is due to the last avalanche, corresponding to catastrophic failure (right). On the left figure we show the same distribution without the last event and with logarithmic bins.

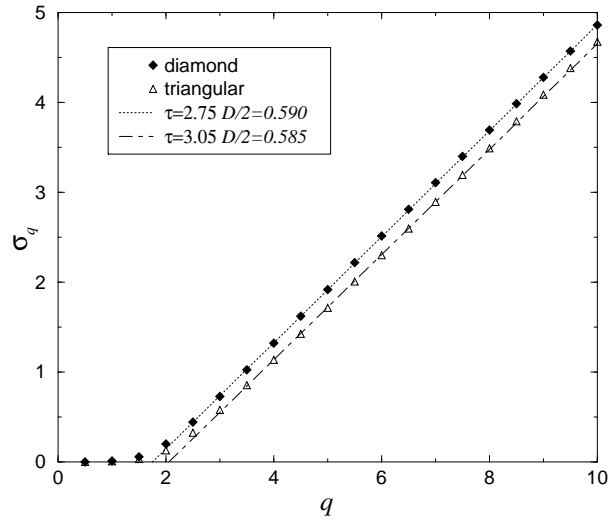


FIG. 7: The exponent σ_q ruling the scaling of the q th moment for triangular and diamond lattice. The shift in the lines indicates a difference in the value of τ .

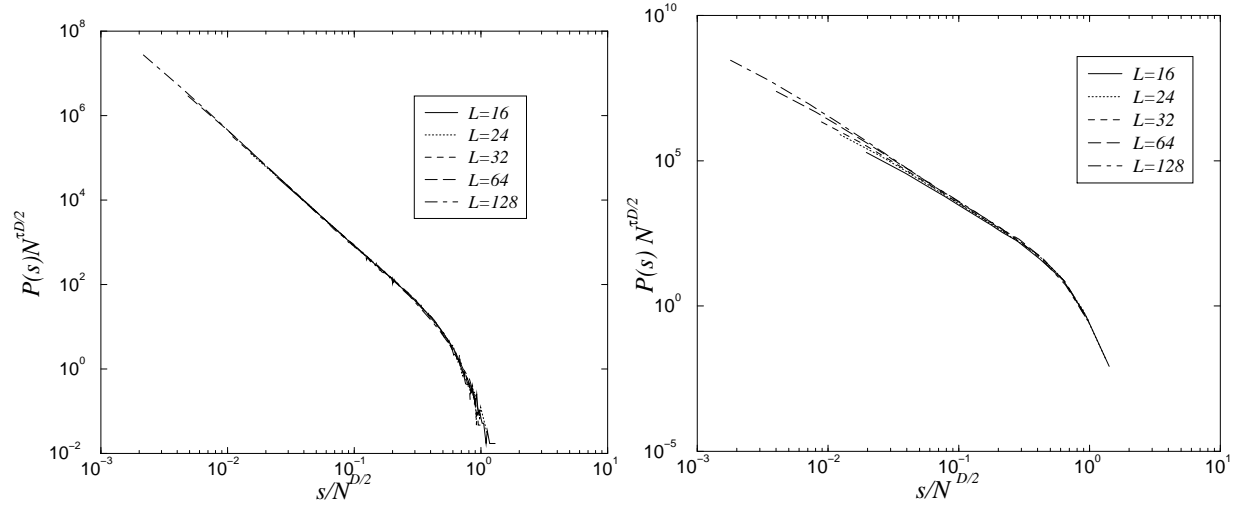


FIG. 8: Data collapse of the avalanche size distributions. The exponent used for the collapse are $\tau = 2.75$ and $D = 1.18$ for the diamond lattice (left) and $\tau = 3.05$ and $D = 1.17$ for the triangular (right) lattice.

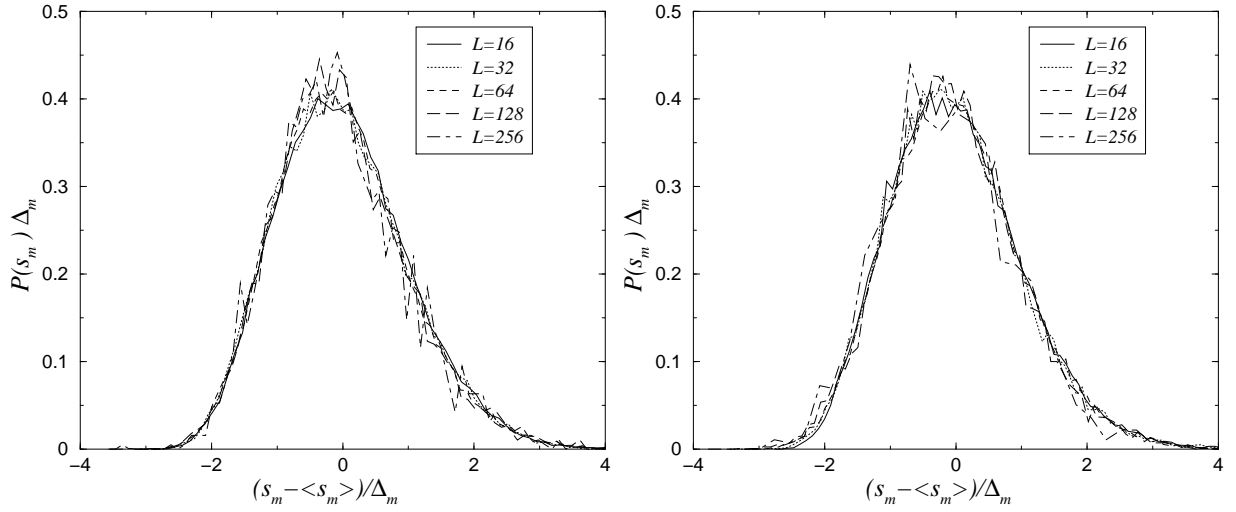


FIG. 9: Data collapse of the distribution of the last avalanche for diamond (left) and triangular (right) lattice.

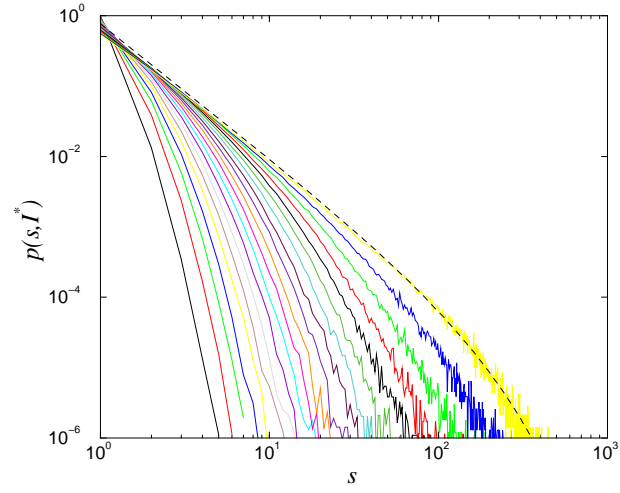


FIG. 10: The avalanche size distributions sampled over a small bin of the reduced current I^* for a diamond lattice of size $L = 128$. The dashed line represents a fit according to Eq. 5 with $\gamma = 1.9$.

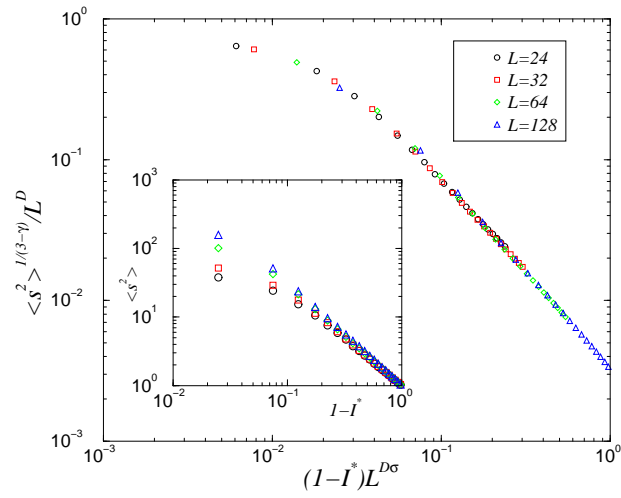


FIG. 11: The second moment of the avalanche size distribution as a function of the reduced current $1 - I^*$ for diamond lattices of different sizes (inset). The curves can be collapsed using the finite size scaling assumption reported in Eq. 6 with $\gamma = 1.9$, $D = 1.18$ and $1/\sigma = 1.4$.